

## Identification of Protein Kinase C Isozymes Responsible for the Phosphorylation of Photoreceptor-specific RGS9-1 at Ser<sup>475</sup>\*

Received for publication, November 19, 2002, and in revised form, December 13, 2002  
Published, JBC Papers in Press, December 23, 2002, DOI 10.1074/jbc.M211782200

Izabela Sokal‡, Guang Hu§, Yan Liang‡, Muling Mao§, Theodore G. Wensel§,  
and Krzysztof Palczewski‡¶||\*\*

From the Departments of ‡Ophthalmology, ¶Pharmacology, and ||Chemistry, University of Washington, Seattle, Washington 98195 and the §Verna and Marrs McLean Department of Biochemistry and Molecular Biology, Baylor College of Medicine, Houston, Texas 77030

Inactivation of the visual G-protein transducin by GTP hydrolysis is regulated by the GTPase-accelerating protein (GAP) RGS9-1. Regulation of RGS9-1 itself is poorly understood, but we found previously that it is subject to a light- and Ca<sup>2+</sup>-sensitive phosphorylation on Ser<sup>475</sup>. Because there are much higher RGS9-1 levels in cones than in rods, we investigated whether Ser<sup>475</sup> is phosphorylated in rods using *Coneless* mice and found that both the phosphorylation and its regulation by light occur in rods. Therefore, we used rod outer segments as the starting material for the purification of RGS9-1 kinase activity. Two major peaks of activity corresponded to protein kinase C (PKC) isozymes, PKC $\alpha$  and PKC $\theta$ . A synthetic peptide corresponding to the Ser<sup>475</sup> RGS9-1 sequence and RGS9-1 were substrates for recombinant PKC $\alpha$  and PKC $\theta$ . This phosphorylation was removed efficiently by protein phosphatase 2A, an endogenous phosphatase in rod outer segments, but not by PP1 or PP2B. Phosphorylation of RGS9-1 by PKC had little effect on its activity in solution but significantly decreased its affinity for its membrane anchor protein and GAP enhancer, RGS9-1 anchor protein (R9AP). PKC $\theta$  immunostaining was at higher levels in cone outer segments than in rod outer segments, as was found for the components of the RGS9-1 GAP complex. Thus, PKC-mediated phosphorylation of RGS9-1 represents a potential mechanism for feedback control of the kinetics of photoresponse recovery in both rods and cones, with this mechanism probably especially important in cones.

Transducin (Gt)<sup>1</sup>, the visual G-protein, is inactivated when its bound GTP is hydrolyzed to GDP, a free phosphate dissoci-

ates from the catalytic site, and the  $\alpha$  subunit reassociates with its partner  $\beta\gamma$  subunits. The rate of hydrolysis is regulated by the protein's association with a GTPase-accelerating protein (GAP). This GAP has been identified to be RGS9-1 (1), a member of a family of regulatory proteins for G $\alpha$  GAPs termed the regulators of G-protein signaling (RGS) family (reviewed in Refs. 2 and 3). The GAP activity of RGS9-1 is further enhanced by the  $\gamma$ -subunit of the phototransduction effector cGMP phosphodiesterase (PDE $\gamma$ ) (1, 4). The acceleration of GTPase activity is essential for timely recovery of dark conditions of photoreceptor cells (5) (for recent reviews, see Refs. 6 and 7).

RGS9-1 contains a G-protein- $\gamma$ -subunit-like domain (8) that is employed for functional association with the G $\beta$ 5L subunit (9–12). This subunit regulates GAP activity by the effector subunit, PDE $\gamma$ , and induces and stabilizes RGS9-1 (5, 10, 13). ROS membranes from knockout mice lacking RGS9 hydrolyze GTP more slowly than ROS membranes from control mice. Moreover, in electrophysiological measurements, the flash responses of *RGS9-/-* rods recovered much more slowly than normal after illumination (5). Alternative splicing of the RGS9 gene yields two molecular forms of RGS9, RGS9-1 and RGS9-2, that vary only in the amino acid sequence of the C terminus. RGS9-1 is a retina-specific transcript, whereas RGS9-2 is expressed in the brain (1, 14, 15). Immunolocalization using monoclonal antibodies and confocal microscopy revealed that RGS9-1 is present in cones at significantly higher levels than in rods, implying that the RGS9-1 level is a potentially important determinant of the faster response kinetics and lower sensitivity of mammalian cones compared with rods (16). RGS9-1 also forms a complex with a 25-kDa photoreceptor-specific phosphoprotein, RGS9-1 anchor protein (R9AP). R9AP binds to the N-terminal domain of RGS9-1 and anchors RGS9-1 to the disk membrane (17).

We previously reported that RGS9-1 is phosphorylated by an endogenous kinase in ROS membranes with an average stoichiometry of 0.2–0.45 mol of phosphates/mol of RGS9-1 (18). A single major site of phosphorylation was identified by a combination of mass spectrometric analysis and mutagenesis as Ser<sup>475</sup>. The kinase responsible has been only partially characterized. Initial studies revealed that the RGS9-1 kinase is a peripheral membrane protein that differs from protein kinase A, protein kinase G, rhodopsin kinase, CaM kinase II, casein kinase II, and cyclin-dependent kinase 5. In addition, it is sensitive to the PKC inhibitor bisindolylmaleimide I. The kinase activity was also inhibited by EGTA and restored by submicromolar [Ca<sup>2+</sup>]. The kinase co-purifies with rhodopsin in sucrose gradients and can be extracted in buffers of high

G-protein signaling; R9AP, RGS9-1 anchor protein; PP1, PP2A, and PP2B, protein phosphatase 1, 2A, and 2B, respectively.

\* This research was supported by National Institutes of Health Grants EY13385 and EY11900, Training Grant EY07001, and Core Grant P30EY0173; the Welch Foundation; a grant from Research to Prevent Blindness, Inc. (RPB) (to the Department of Ophthalmology at the University of Washington); and a grant from the E. K. Bishop Foundation. The costs of publication of this article were defrayed in part by the payment of page charges. This article must therefore be hereby marked "advertisement" in accordance with 18 U.S.C. Section 1734 solely to indicate this fact.

\*\* An RPB Senior Investigator and a recipient of the Humboldt Research Award for Senior United States Scientists. To whom correspondence should be addressed: Dept. of Ophthalmology, University of Washington, Box 356485, Seattle, WA 98195-6485. Tel.: 206-543-9074; Fax: 206-221-6784; E-mail: palczewski@u.washington.edu.

<sup>1</sup> The abbreviations used are: Gt, G-protein transducin; BTP, 1,3-Bis[tris(hydroxymethyl)methylamino]propane; CaM, calmodulin; DAG, diacylglycerol; GAP, GTPase-accelerating protein(s); MOPS, 4-morpholinopropanesulfonic acid; PDE, phosphodiesterase; PKA, cAMP-dependent protein kinase; PKC, protein kinase C; PKG, cGMP-dependent protein kinase; PMA, phorbol 12-myristate 13-acetate; PS, phosphatidylserine; ROS, rod outer segment(s); RGS, regulator(s) of

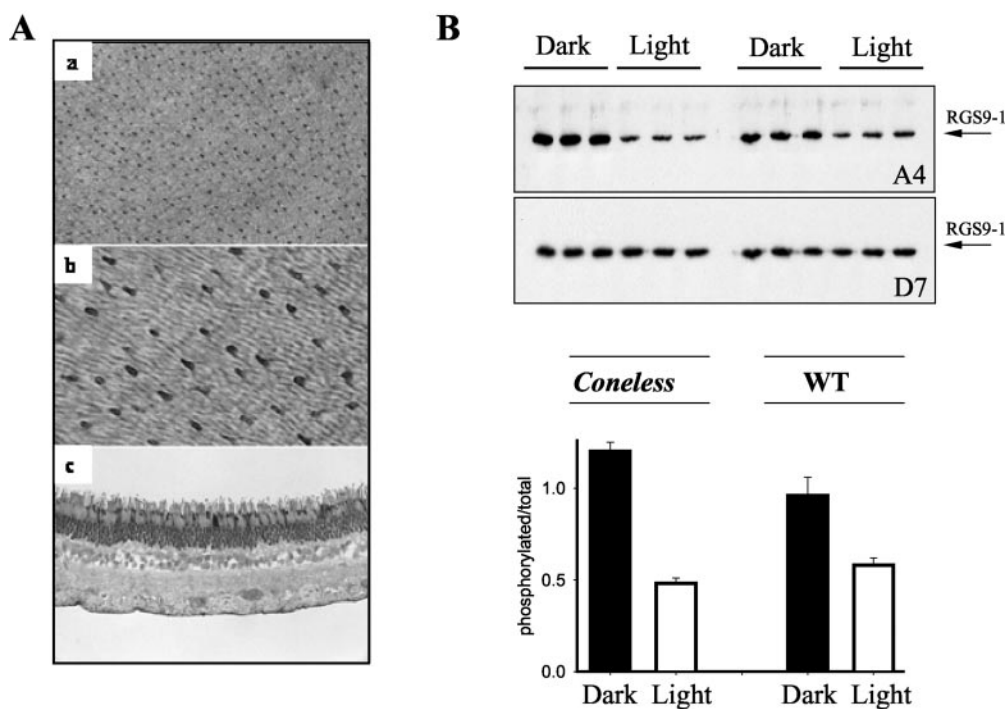


FIG. 1. **Localization of RGS9-1 in rod and cone photoreceptors and its phosphorylation *in vivo*.** *A*, flat mount immunolocalization of RGS9-1 in bovine retina using the D7 monoclonal antibody. Lower (*a*) and higher (*b*) magnifications, respectively, and a cross-section of the bovine retina (*c*) are shown. Cones (more prominently) and rods were immunolabeled. *B*, phosphorylation of RGS9-1 in dark- and light-adapted wild type and *Coneless* mouse retinas. RGS9-1 was immunoprecipitated from dark-adapted (*Dark*) or light-adapted (*Light*) mouse retinas and immunoblotted with Ser<sup>475</sup> phosphate-specific antibody (A4 antibody). RGS9-1 phosphorylation under different conditions was compared as described under "Materials and Methods."

ionic strength (18). We also developed a monoclonal antibody specific for the Ser<sup>475</sup>-phosphorylated form of RGS9-1 and found that it recognized RGS9-1 in immunoblots of dark-adapted mouse retina (18). Retinas from light-adapted mice had much lower levels of RGS9-1 phosphorylation. Thus, RGS9-1 is phosphorylated on Ser<sup>475</sup> *in vivo*, and the phosphorylation level is regulated by light and by [Ca<sup>2+</sup>], suggesting the importance of the modification in light adaptation. Phosphorylated RGS9-1 is present exclusively in the cholesterol-rich detergent-insoluble membrane domains (Rafts), whereas the unphosphorylated form can be readily extracted with mild detergent (19). These results demonstrate differences in the subcellular localization between phosphorylated RGS9-1 and its unphosphorylated form.

In another study, cAMP-dependent protein kinase (PKA) inhibitor H89 reduced RGS9-1 phospholabeling by more than 90%, whereas dibutyryl-cAMP stimulated it 3-fold (20). These studies suggested PKA as the major kinase responsible for RGS9-1 phosphorylation in ROS. The PKA catalytic subunit was found to phosphorylate recombinant RGS9-1, and mutational analysis of a fragment of RGS9 (residues 276–431) identified the phosphorylation sites as Ser<sup>427</sup> and Ser<sup>428</sup>. However, in ROS, RGS9-1 phosphorylation required the presence of free Ca<sup>2+</sup> ions and was inhibited by light (20).

The current work focused on the identification of the protein kinase(s) and the protein phosphatase responsible for regulating phosphorylation of RGS9-1. We used bovine ROS as a starting material and carefully fractionated protein kinase activities, quantitatively accounting for the RGS9-1 kinase activity. We report here that two PKC isozymes from ROS, PKC $\alpha$  and PKC $\theta$ , co-purify with RGS9-1 kinase activity, that both phosphorylate RGS9-1 at Ser<sup>475</sup>, and that protein phosphatase 2A is responsible for the RGS9-1 dephosphorylation at this site.

#### MATERIALS AND METHODS

**Proteins**—Recombinant kinases, phosphatases, and antibodies were purchased as follows: PKA and PKC $\alpha$  from Sigma; PKGI, anti-PKGI antibody, and Ca<sup>2+</sup>/CaM II kinase from Calbiochem; PKC $\theta$  and PKC $\epsilon$  from PanVera; PP1 and PP2A phosphatases from Upstate Biotechnology, Inc. (Lake Placid, NY); and PP2B and CaM from Biomol. Fluorescein-labeled peanut agglutinin (PNA) was from Vector Laboratory Inc.

**Anti-RGS Antibodies**—Monoclonal antibody D7 was raised against bacterially expressed RGS9-1 as described previously (16). Mouse anti-phosphorylated RGS9-1 monoclonal antibody (A4) was raised against a C-terminal peptide derived from mouse phosphorylated RGS9-1, (KLDRRpSQLKKELPPK, where pS represents phosphorylated serine); Quality Controlled Biochemicals, Inc., Hopkinton, MA), and coupled to a carrier protein, keyhole limpet hemocyanin (Sigma) (18). Rabbit anti-RGS9-1c polyclonal serum was generated as described previously (1).

**Expression and Purification of Recombinant RGS9-1 and R9AP**—RGS9-1 proteins, with either a glutathione *S*-transferase or His<sub>6</sub> tag on the N terminus, bound to G $\beta$ 5 were expressed using baculovirus and Sf9 cells, as described previously (10, 18), and affinity-purified using either immobilized metal or glutathione affinity chromatography. The RGS9-1 membrane anchor protein, R9AP, with an N-terminal His<sub>6</sub> tag, was expressed in *Escherichia coli* and purified, as described elsewhere.<sup>2</sup>

**Phosphorylation of RGS9-1 *in Vivo***—All animal experiments employed procedures approved by the University of Washington Animal Care Committee and conformed with recommendations of the American Veterinary Medical Association Panel on Euthanasia. All animals were maintained in complete darkness, and all manipulations were done under dim red light employing Kodak number 1 safelight filters (transmittance >560 nm). *Coneless* mice were obtained from J. Nathans (Johns Hopkins University) and GCAP1/2 knockout mice from J. Chen (Southern California University). The analysis of RGS9-1 phosphorylation of mouse retinas was carried out essentially as described previously (18). Briefly, mice were maintained in a dark room (dark-adapted) or in full room light (light-adapted) for a period of 16 h prior to euthanasia and removal of retinas under dim red light. The retinas were homogenized with 10 mM Tris-HCl, 100 mM NaCl, 2 mM MgCl<sub>2</sub>, ~20

<sup>2</sup> Hu, G., Zhang, Z., and Wensel, T. G. (January 30, 2003) *J. Biol. Chem.* 10.1074/jbc.m212046200.

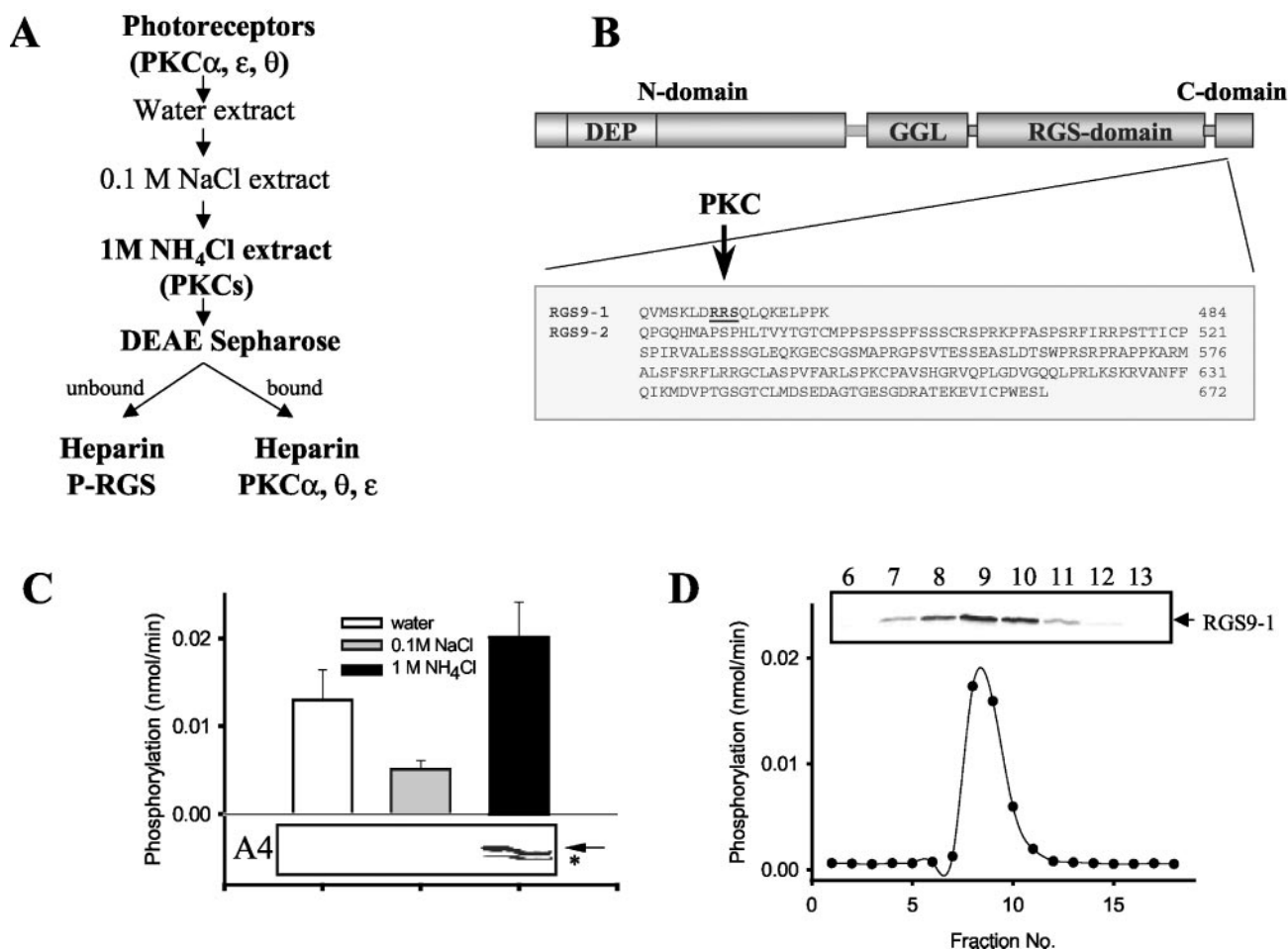


**FIG. 2. Schematic representation of RGS9 and extraction of RGS9-1 kinase and the DEAE-Sepharose chromatography of the NH<sub>4</sub>Cl extract from bovine ROS.** *A*, flowchart of RGS9-1 kinase purification from ROS. Hydroxyapatite chromatography is not included, since it did not separate RGS9-1 kinase activities. *B*, the scheme represents DEP (protein interaction), G-protein  $\gamma$ -subunit-like (*GGL*), and RGS domains of RGS9. The C-terminal region of human RGS9-1 and human RGS9-2 are aligned, and the unique phosphorylation sequence in RGS9-1 is highlighted. The sequence of human RGS9-1 was previously published (14), and the sequence of human RGS9-2 was obtained from GenBank™ (accession number AF071475). *C*, extraction of the RGS9-1 kinase activity from bovine ROS with H<sub>2</sub>O, 0.1 M NaCl, or 1 M NH<sub>4</sub>Cl. The RGS9-1 kinase activity was assayed using a synthetic peptide that encompassed the identified Ser<sup>475</sup> phosphorylation site (KLDRRS<sup>475</sup>QLKKGLPPK) by the phosphocellulose method (*graph*), or by immunoblot (*inset*) using Ser<sup>475</sup> phosphate-specific antibody (A4 antibody) as described under "Materials and Methods." The *arrow* indicates phosphorylation of recombinant RGS9-1, whereas the *asterisk* represents endogenous phosphorylated RGS9-1. *D*, DEAE-Sepharose chromatography. The activity profile of RGS9-1 kinase from the DEAE-Sepharose column was measured using the RGS9-1 peptide assay. *Inset*, the RGS9-1 kinase activity was probed with A4 antibody using recombinant RGS9-1.

mg/liter phenylmethylsulfonyl fluoride with 1% Nonidet P-40 detergent, plus 0.2 mM Na<sub>3</sub>VO<sub>4</sub>, 15  $\mu$ M fenvalerate, and 100 nM okadaic acid to inhibit phosphatase activities. Immunoprecipitation of RGS9-1 was carried out using rabbit polyclonal antibodies (18), and the immunoprecipitated protein was analyzed by SDS-PAGE and immunoblotting with the mouse monoclonal antibody A4 specific for the phosphopeptide and phosphorylation-independent antibody D7 at a dilution of 1:500. The secondary antibody used was horseradish peroxidase-conjugated (Promega), and detection was done by chemiluminescence using the ECL® system (Amersham Biosciences). RGS9-1 phosphorylation was compared between dark- and light-adapted animals by densitometry of films. Three data points from immunoblots were averaged, and relative phosphorylation levels were calculated as follows: relative RGS9-1 phosphorylation = (average densities of RGS9-1 bands in Ser<sup>475</sup>-phosphate-specific antibody immunoblots)/(average densities of RGS9-1 bands in monoclonal anti-RGS9-1 antibody D7 immunoblots). Phosphorylation levels were normalized to the relative phosphorylation value obtained in wild type mice.

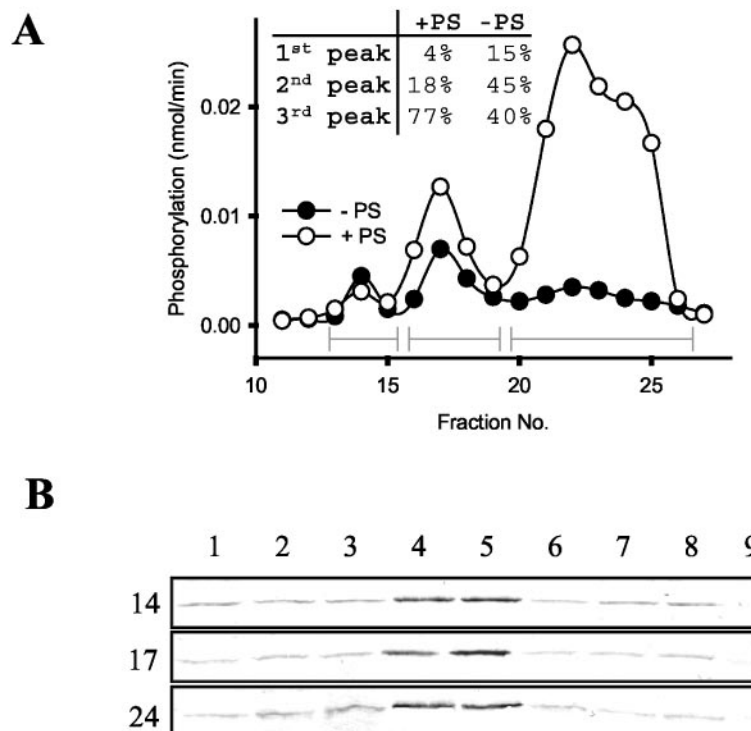
**Kinase Assays for Kinase Purification and Characterization**—The RGS9-1 kinase activity was routinely assayed using the KLDRRS<sup>475</sup>QLKKGLPPK peptide derived from the C-terminal region of RGS9-1 that is phosphorylated *in vitro* in ROS suspensions (18). This site is also phosphorylated in RGS9-1 *in vivo* (18). In the standard conditions, phosphorylation was carried out in 10 mM BTP, pH 7.5, 5 mM MgCl<sub>2</sub>, containing 13 mg/ml peptide with and without 0.1 mM cGMP, 0.1 mM cAMP, 0.01 mM DAG, 1 mM PMA, 50 mM Ca<sup>2+</sup>, 50 mM EGTA, 3  $\mu$ M CaM,

and 230 mg/ml PS. The phosphorylation reaction was initiated by an addition of [ $\gamma$ -<sup>32</sup>P]ATP to a final concentration of 0.1 mM with a specific activity of 100,000 dpm/nmol and a total volume of 75  $\mu$ l. Samples were incubated for 10 min or a longer time as indicated, at 30 °C. The reaction was stopped by the addition of 20  $\mu$ l of 100 mM H<sub>3</sub>PO<sub>4</sub>. <sup>32</sup>P incorporation into the RGS peptide was determined by a phosphocellulose filter paper method (21).

Alternatively, qualitative assays of RGS9-1 kinase activity were carried out using similar conditions as described for the peptide assays, using the recombinant His<sub>6</sub>-RGS9-1/G $\beta$ 5-subunit complex as a substrate, and phosphorylation was detected using the A4 antibody specific for Ser<sup>475</sup> phosphorylation.

**Phosphorylation of RGS9-1 by Recombinant PKC for Functional Assays**—His<sub>6</sub>- or glutathione *S*-transferase-tagged RGS9-1 full-length protein with G $\beta$ 5L was affinity-purified from insect Sf9 cells as described (10). *In vitro* phosphorylation assays were performed in kinase buffer (20 mM MOPS, pH 7.2, 1 mM NaF, 1 mM MgCl<sub>2</sub>, 1 mM Na<sub>3</sub>VO<sub>4</sub>, 1 mM dithiothreitol, 500  $\mu$ M ATP) containing either 1 mM CaCl<sub>2</sub> for PKC $\alpha$  or 1 mM EDTA for PKC $\theta$ . PS (0.1 mg/ml) and DAG (0.01 mg/ml, Upstate Biotechnology) were added after sonication on ice for 2 min to resuspend the lipid micelles. Either PKC $\alpha$  (60 ng) or PKC $\theta$  (60 milliunits) was used in the assay, unless otherwise indicated. For autoradiography, [ $\gamma$ -<sup>32</sup>P]ATP was added with a working concentration of 200 Ci/mol. The reactions were performed at 30 °C for 60 min or as indicated, and then either diluted directly into GAP assay reactions for GAP activity measurement or quenched by SDS sample buffer for SDS-PAGE. Incorpora-

**FIG. 3. Heparin-Sepharose chromatography.** Fractions eluted from the DEAE-Sepharose column were loaded onto the heparin-Sepharose column, and the RGS9-1 kinase activity was measured as described under "Materials and Methods." **A**, phosphorylation of RGS9-1 peptide in the presence and absence of PS. *Inset*, the RGS kinase activity, eluted in three peaks, as a percentage of total activity with or without PS. **B**, enzyme activity was assayed in the absence (*lane 1*) and presence of cGMP (*lane 2*); cAMP (*lane 3*); DAG, PS, and  $\text{Ca}^{2+}$  (*lane 4*); PS, PMA, and  $\text{Ca}^{2+}$  (*lane 5*); CaM and  $\text{Ca}^{2+}$  (*lane 6*);  $\text{Ca}^{2+}$  (*lane 7*); EGTA (*lane 8*) or peptide (*lane 9*) as described under "Materials and Methods." *Lane 9*, the reaction without the addition of any fraction. The RGS9-1 kinase activity was probed with A4 antibody using recombinant RGS9-1



of  $^{32}\text{P}$  into RGS9-1 after kinase assays was determined by autoradiography after separating the proteins by SDS-PAGE, and the phosphorylation on Ser<sup>475</sup> was determined by immunoblotting using Ser<sup>475</sup> phosphorylation-specific A4 antibody. Reactions without PKC kinases were used as negative controls.

**Purification of RGS9 Kinase**—ROS were purified in dim red light from fresh or frozen bovine retinas as described (22). All procedures were performed on ice or at 4 °C. Bovine ROS (obtained from 200 retinas) were homogenized with 50 ml of water, and the membranes were collected by centrifugation at  $100,000 \times g$  for 20 min. The water extraction was repeated a second time, and two additional extractions were performed in 10 mM BTP, pH 7.5, containing 100 mM NaCl. RGS kinase(s) was extracted using 10 mM BTP, pH 7.5, containing 1 M  $\text{NH}_4\text{Cl}$ . The high salt extraction was repeated twice, and the obtained supernatants were combined (~150 ml) and loaded onto hydroxyapatite (1.5 ml) at a flow rate of 15 ml/min. The column was washed with 300 mM NaCl in 10 mM BTP, pH 7.5, and proteins containing the RGS9-1 kinase activity were eluted with 300 mM  $\text{K}_2\text{HPO}_4$  in 10 mM BTP, pH 7.5. Salt was removed by dialysis against 10 mM BTP, pH 7.5, and proteins were chromatographed on a DEAE-Sepharose (5 ml; Amersham Biosciences) column pre-equilibrated with 10 mM BTP, pH 7.5, at a flow rate of 0.8 ml/min. Unbound proteins were removed by 10 mM BTP buffer, pH 7.5, whereas remaining proteins were eluted with a linear gradient of 0–1 M NaCl in 10 mM BTP buffer, pH 7.5. Fractions with kinase activity were pooled together, dialyzed, and applied to a heparin-Sepharose column previously equilibrated with 10 mM BTP, pH 7.5. Proteins were eluted with a linear gradient of 0–0.4 M NaCl in 10 mM BTP, pH 7.5. RGS9-1 kinase activity was monitored using the peptide or recombinant RGS9-1 immunoblot assays as described above.

**PKGII Expression**—HEK cells at 40% confluence in 10-cm plates were transfected by calcium phosphate precipitation with 20  $\mu\text{g}$ /plate of pCMV.CGKII (a gift from M. Uhler) (23). After 26 h, the cells were washed with PBS buffer, scraped, and homogenized. Expression of the enzyme was confirmed by immunoblot using anti-PKGII (M. Uhler).

**P-RGS Dephosphorylation**—Dephosphorylation was carried out for 20 min at 30 °C in 15  $\mu\text{l}$  of 10 mM BTP pH 7.5, with the addition of 0.4 units of phosphatase, 5 mM  $\text{MgCl}_2$ , and 5  $\mu\text{g}$  of bovine ROS. The reaction was quenched by the addition of SDS-PAGE sample buffer. After separation in SDS-PAGE gels, dephosphorylation/phosphorylation was visualized by immunoblot and A4 antibody.

**SDS-PAGE and Immunoblotting**—SDS-PAGE was performed according to Laemmli (24) with 12% polyacrylamide gels. For immunoblotting, membranes were blocked with 2% bovine serum albumin in 20 mM Tris, pH 8.0, containing 150 mM NaCl and 0.05% Tween 20 and incubated for 1 h with primary antibodies (D7 and A4), 1:1000 or 1:500. When secondary antibody conjugated with alkaline phosphatase (Pro-

mega) was used, the dilution was 1:7000, and antibody binding was detected using 5-bromo-4-chloro-3-indolyl phosphate and nitro blue tetrazolium as a substrate. When secondary antibody conjugated with horseradish peroxidase (Promega) was used, the dilution was 1:5000, with detection by chemiluminescence using the ECL<sup>®</sup> system (Amersham Biosciences).

**Immunolocalization**—For flat mount localization, bovine eyes obtained from a local slaughterhouse were held briefly on ice prior to dissection. For localization in mouse and bovine retinas, the anterior segment and vitreous humor were removed from each eye, and the eye cups were immersed for 6 h in chilled 4% formaldehyde in 0.086 M sodium phosphate buffer, pH 7.3. Pieces of retina (5 mm<sup>2</sup>) were excised, washed in phosphate buffer, and embedded in 5% agarose in phosphate-buffered saline. Sections of retina (100  $\mu\text{m}$  thick) were cut with a VT1000E vibrating microtome (Leica). Antibody labeling was assessed by indirect immunofluorescence. Sections were first incubated in normal goat serum diluted 1:50 in ICC buffer (phosphate-buffered saline containing 0.5% bovine serum albumin, 0.2% Triton X-100, and 0.05% sodium azide, pH 7.3) for 1 h to reduce nonspecific labeling. Mouse monoclonal RGS9 antibody ( $A_{280} = 0.69$ ) diluted 1:25 in ICC buffer was added to retinal sections for incubation overnight in a humidified chamber. Negative controls for antibody labeling were produced by omitting primary antibody from the incubation buffer or by preadsorbing RGS9 antibody with purified full-length RGS9 coupled to CNBr-activated Sepharose (0.5 ml, 1 mg/ml RGS9). After repeated washing in buffer, sections were incubated for 4 h in indocarbocyanine (Cy3)-conjugated goat anti-mouse antibody (Jackson ImmunoResearch, Inc.) diluted 1:200 in ICC buffer. Sections were washed repeatedly with ICC buffer, mounted in 5% *n*-propyl gallate in glycerol, coverslipped, and examined on a Bio-Rad MRC 600 laser-scanning confocal microscope. Scan head parameters influencing image intensity and resolution (pinhole aperture, PMT gain and black level, and attenuation of laser by neutral density filters) were standardized for all samples. Single plane and Z series images were collected and stored as unprocessed files. Images for publication were processed with Adobe Photoshop 3.0.

**Single-turnover GTPase Assays**—Single-turnover GTPase assays were performed as described previously (1, 25). PKC-phosphorylated or -unphosphorylated RGS9-1 were mixed with urea-washed ROS, purified Gt, PDE $\gamma$ , and [ $\gamma$ - $^{32}\text{P}$ ]GTP to measure GAP activity. Final concentrations of the proteins in the assays were as follows: 0.5  $\mu\text{M}$  RGS9-1/G $\beta$ 5, 15  $\mu\text{M}$  rhodopsin, 1  $\mu\text{M}$  Gt, and 2  $\mu\text{M}$  PDE $\gamma$ . The first order rate constant for GTP hydrolysis was calculated by fitting data with PSI-Plot.

**RGS9-1 Binding to R9AP Vesicles**—The binding assays were carried out as described recently.<sup>2</sup> *E. coli* expressed His<sub>6</sub>-R9AP was purified in detergent and reconstituted into lipid vesicles containing L- $\alpha$ -phos-

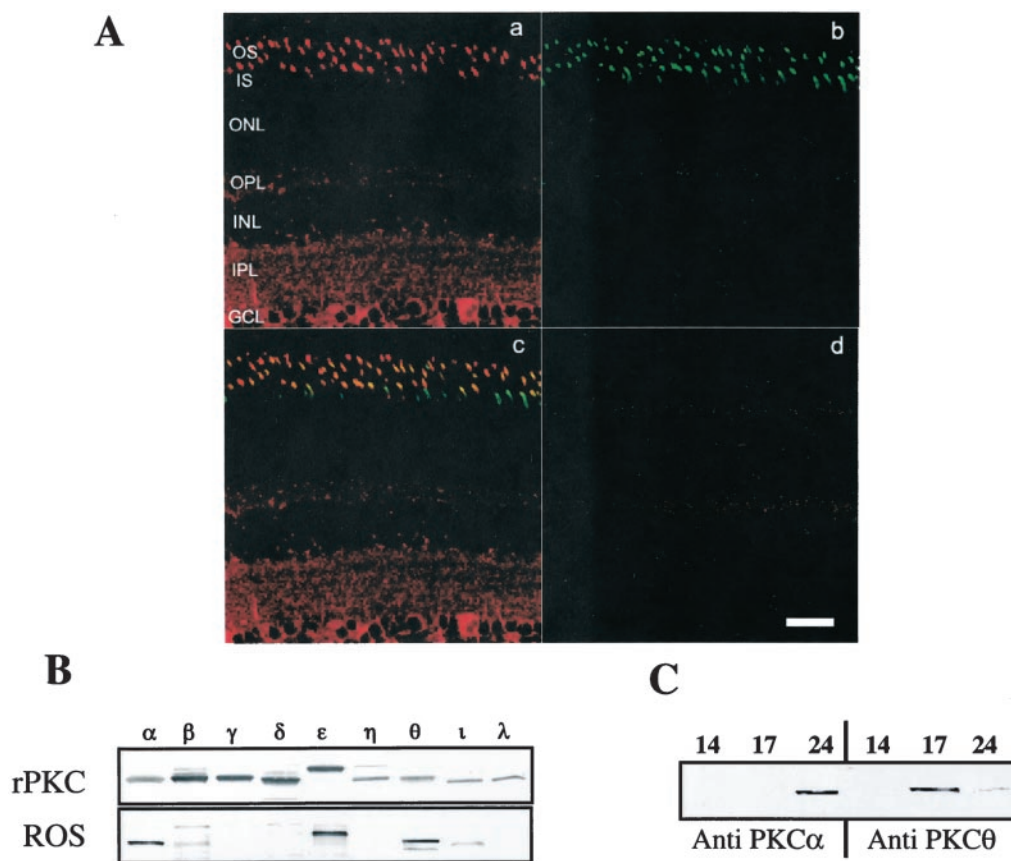


**FIG. 4. Immunofluorescence localization and immunoblotting analysis of PKC isozymes in the retina.** *A*, immunofluorescence localization of the PKC $\theta$  isozyme in mouse retina. Cones, but not rods, were strongly immunolabeled with anti-PKC $\theta$ -specific antibody (*a*, red), and anti-peanut agglutinin antibody labeled cone extracellular matrix (*b*, green). Both immunolabelings coincide as shown by double labeling (*c*, yellow). PKC $\theta$  immunolabeling is abolished by preadsorbing antibody on the PKC $\theta$  peptide antigen (*d*). Scale bars, 20  $\mu$ m. The retinal layers are as follows: OS, outer segment layer; IS, inner segment layer; ONL, outer nuclear layer; OPL, outer plexiform layer; INL, inner nuclear layer; IPL, inner plexiform layer; GCL, ganglion cell layer. *B*, identification of PKC isozymes in the bovine ROS preparations. The specificity of each antibody was tested using recombinant PKC isozymes (*rPKC*). *C*, immunoblot of fractions 14, 17, and 24 with anti-PKC $\alpha$  and anti-PKC $\theta$  antibodies.

phatidylserine (PS; brain, porcine-sodium salt), L- $\alpha$ -phosphatidylcholine (egg, chicken), L- $\alpha$ -phosphatidylethanolamine (egg, chicken) (Avanti Polar Lipids) at a ratio (w/w/w) of L- $\alpha$ -phosphatidylcholine/L- $\alpha$ -phosphatidylethanolamine/PS = 50:35:15 as described. Rhodamine-labeled L- $\alpha$ -phosphatidylethanolamine (*N*-(6-tetramethylrhodaminethiocarbonyl)-1,2-dihexadecanoyl-*sn*-glycero-3-phosphoethanolamine, triethylammonium salt; Molecular Probes, Inc., Eugene, OR) was added in the lipid mixture to a final concentration of 0.5% (w/w) to facilitate the visualization of the lipids. Purified glutathione *S*-transferase-RGS9-1/G $\beta$ 5 proteins (in 10 mM HEPES, pH 7.4, containing 100 mM NaCl and 2 mM MgCl<sub>2</sub>) were first incubated with buffer only or phosphorylated by commercial PKC $\alpha$  or PKC $\theta$  at room temperature for 60 min and then centrifuged at 4  $^{\circ}$ C at 88,000  $\times$  *g* for 40 min to remove aggregates. Supernatants were diluted to desired concentrations in 10 mM HEPES, pH 7.4, containing 100 mM NaCl, 2 mM MgCl<sub>2</sub> and 0.2 mg/ml ovalbumin, mixed with R9AP vesicles in a volume of 150  $\mu$ l, and incubated with gentle vortexing at 4  $^{\circ}$ C for  $\sim$ 2 h. An aliquot (100  $\mu$ l) of the reaction mixture was then transferred to a new polypropylene (Beckman) tube to separate unbound proteins from bound proteins by pelleting the vesicles at 88,000  $\times$  *g* for 40 min. The pelleted vesicles were clearly visible as a pink pellet at the bottom of the tube due to the rhodamine-labeled phosphatidylethanolamine. The final concentrations in the binding reactions were as follows: RGS9-1, 0.1  $\mu$ M; R9AP (total concentration), 1.0  $\mu$ M. Equal proportions of the starting binding reactions, the supernatant after pelleting the vesicles, and the pelleted vesicles were loaded on SDS-PAGE, and the RGS9 proteins were detected by immunoblotting using anti-RGS9-1c antiserum.

#### RESULTS

**RGS9-1 Phosphorylation in Transgenic Mice**—RGS9-1 localizes in rod and cone photoreceptors in the bovine retina (16). Previously, we showed that RGS9-1 is phosphorylated in ROS preparations (18). We reinvestigated localization of RGS9-1

using the D7 antibody raised against bacterially expressed RGS9-1 and the flat mount section of bovine retina. The flat mount immunolocalization revealed a significantly higher level of RGS9-1 in cones rather than in rods as shown at lower (Fig. 1*Aa*) and higher magnification (Fig. 1*Ab*). Immunolabeling of RGS9-1 using the cross-section confirmed higher cone expression (Fig. 1*Ac*). Preincubation with purified protein abolished RGS9-1 immunoreactivity (data not shown).

Because of the higher expression levels of RGS9-1 in cone photoreceptors, we sought additional proof that RGS9-1 is phosphorylated in ROS. One possible explanation for our previous results on RGS9-1 phosphorylation in ROS was that isolated ROS were contaminated by RGS9-1 from cone outer segments, where it is highly enriched, and consequently, phosphorylation was a cone-specific phenomenon. Therefore, to evaluate RGS9-1 phosphorylation in rods, we employed mice lacking cone photoreceptors (*Coneless* mice) (26). RGS9-1 immunoprecipitated from retinal homogenates obtained from dark- and light-adapted wild type and *Coneless* mice was subjected to electrophoresis, transferred to Immobilon membrane, and probed for RGS9-1 phosphorylation with the Ser<sup>475</sup> phosphate-specific antibody A4 (18). Immunoblotting with the D7 anti-RGS9-1 antibody revealed that the total amount of immunoprecipitated RGS9-1 was similar in wild type and *Coneless*, as well as in light- and dark-adapted mice (Fig. 1*B*). Comparison of the phosphorylation level between dark- and light-adapted mice revealed that light reduced phosphorylation by  $\sim$ 50% in both wild type and *Coneless* mouse retina (Fig. 1*B*).

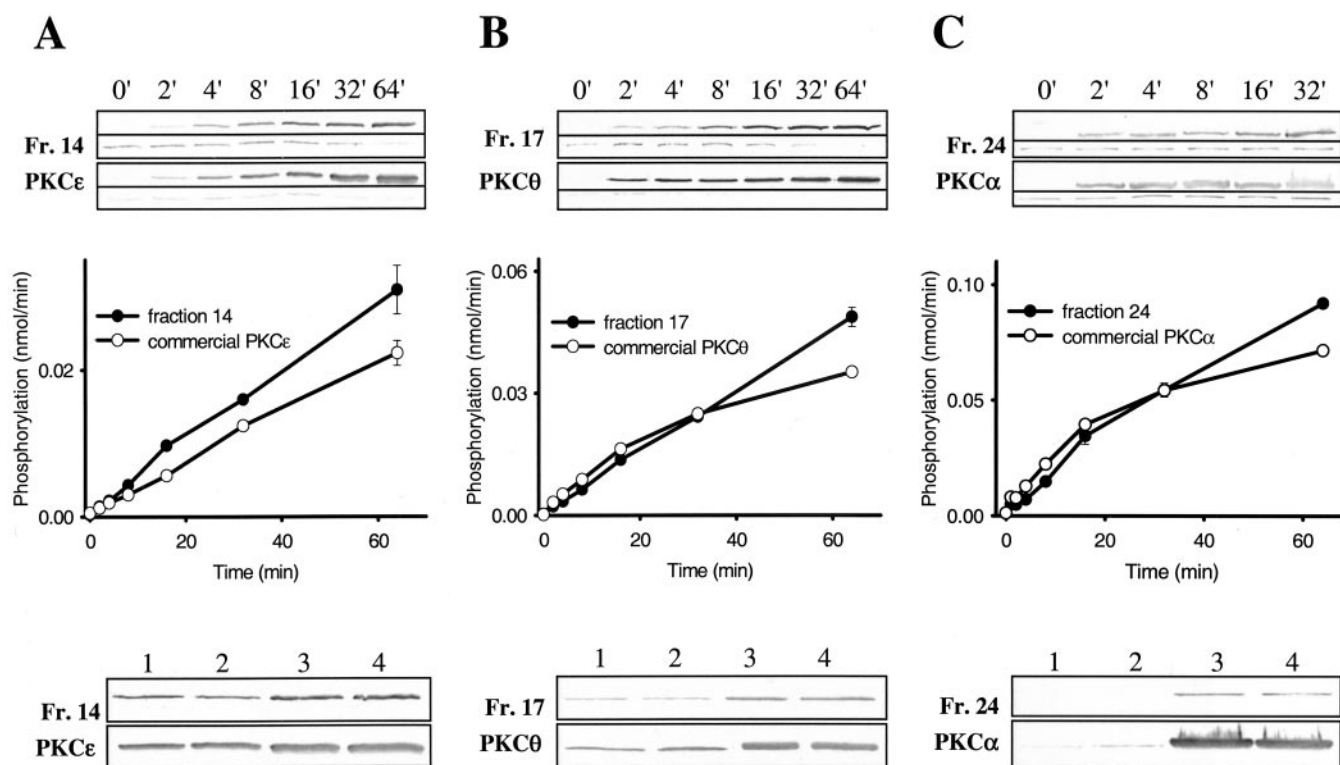


**FIG. 5. RGS9-1 phosphorylation by kinases present in fractions obtained from the heparin-Sepharose column and by recombinant PKC isozymes.** A, time course of RGS9-1 phosphorylation by kinase present in fraction 14 and by recombinant PKC $\epsilon$ . The RGS9-1 kinase activity was assayed by immunoblot using Ser<sup>475</sup> phosphate-specific antibody and recombinant RGS9-1 (upper immunoblot) or using a synthetic peptide that encompassed the identified Ser<sup>475</sup> phosphorylation site (KLDRRS<sup>475</sup>QLKKGLPPK) (graph) as described under "Materials and Methods." Lower panels, the enzyme activities were assayed in the absence (lane 1) and presence of DAG and Ca<sup>2+</sup> (lane 2); PS and Ca<sup>2+</sup> (lane 3); and DAG, PS, and Ca<sup>2+</sup> (lane 4) by immunoblot using Ser<sup>475</sup> phosphate-specific antibody and recombinant RGS9-1 (see "Materials and Methods"). B, time course of RGS9-1 phosphorylation by kinase present in fraction 17 and by recombinant PKC $\theta$ . C, time course of RGS9-1 phosphorylation by kinase present in fraction 24 and by recombinant PKC $\alpha$ . Lower bands in the upper panels represent RGS9-1 immunoblot with D7 monoclonal antibody as a control of the loading on the gel.

These results demonstrate that RGS9-1 phosphorylation occurs in rod cells *in vivo* and is regulated by light.

Because RGS9-1 phosphorylation is regulated *in vitro* by Ca<sup>2+</sup>, we also measured RGS9-1 phosphorylation in mice lacking GCAP1/GCAP2, two Ca<sup>2+</sup>-binding proteins in photoreceptors (27, 28). We found similar results in those mice as compared with wild type mice, suggesting that GCAP1 and GCAP2 are not involved in the regulation of RGS9-1 phosphorylation (data not shown).

**Extraction of RGS9-1 Kinase**—To identify protein kinases responsible for phosphorylation of RGS9-1 at Ser<sup>475</sup>, bovine ROS was fractionated, and the kinase activity was quantitatively assessed. ROS were used as starting material, because they are readily accessible for biochemical procedures. Two specific assays were utilized to determine RGS9-1 kinase activity. The first assay involves phosphorylation of full-length recombinant RGS9-1 obtained from Sf9 cells, in a complex with G $\beta$ 5, followed by separation of the phosphorylated products on SDS gel and identification and quantification of the phosphorylation by monoclonal anti-Ser<sup>475</sup>-phosphate-specific antibody (A4) (18). The advantage of this method is its ability to recognize the specific phosphorylation on the *in vivo* phosphorylation site Ser<sup>475</sup>, regardless of other nonspecific phosphorylations that could result from high kinase concentrations or missing regulatory components in *in vitro* assays. The second method involves phosphorylation of a synthetic peptide that encompasses the RGS9-1 phosphorylation site identified *in vivo*, KLDRRS<sup>475</sup>QLKKGLPPK (18), using [ $\gamma$ -<sup>33</sup>P]ATP as a phosphoryl donor. The phosphorylation product is trapped on phosphocellulose filter paper and then quantified by scintillation counting. Advantages of this filter paper assay over the

immunoassay include the ability to quantitatively measure kinase activity in a large number of samples. In our study, we measured RGS9-1 kinase activity in ROS extracts using both of the two methods.

Fractionation of RGS9-1 kinase was accomplished by washing bovine ROS membranes with H<sub>2</sub>O, 0.1 M NaCl, and 1 M NH<sub>4</sub>Cl (Fig. 2A). RGS9-1 peptide was phosphorylated by all three extracts, with the highest phosphorylation level by the H<sub>2</sub>O extract (Fig. 2C). However, the specific full-length RGS9-1 kinase activity was found only in the 1 M NH<sub>4</sub>Cl extract using the A4-site-specific antibody. The two phosphorylated bands detected in the A4 immunoblot corresponded to the tagged recombinant (rRGS9-1) and the endogenous RGS9-1 (Fig. 2C, inset). These data indicated that ~38% of the total kinase activity toward the peptide was RGS9-1 specific, tightly membrane associated, and could be extracted with 1 M NH<sub>4</sub>Cl. We also observed that another 32% of the total activity, which remained in the H<sub>2</sub>O and 0.1 M NaCl fractions, was not RGS9-1 specific and could be easily removed during the extraction process. The remaining ROS pellet contained ~30% RGS9-1 kinase activity, which was refractory to all of the above extraction procedures (data not shown).

**Purification of RGS9-1 Kinase from ROS**—RGS9-1 kinase extracted from the ROS membranes with 1 M NH<sub>4</sub>Cl was routinely chromatographed on hydroxyapatite (data not shown) followed by DEAE-Sepharose. From the DEAE-Sepharose column, the bulk of the activity was eluted by a salt gradient as a single peak (Fig. 2D). Fractions 7–11 contained a majority of the RGS9-1 kinase activity (Fig. 2D). This chromatography also separated the RGS9-1 kinase(s) from the endogenously phosphorylated RGS9-1, which did not bind to DEAE-Sepharose

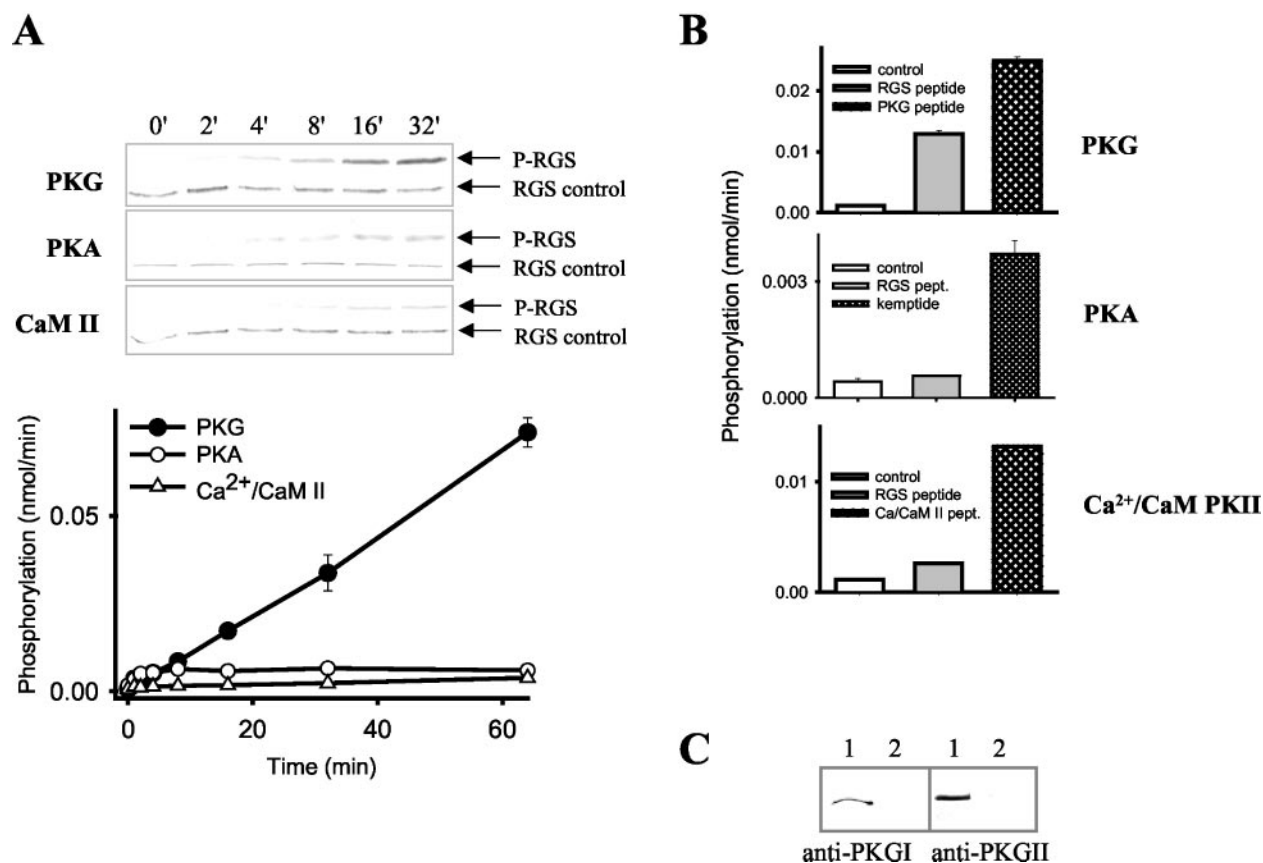


**FIG. 6. RGS9-1 phosphorylation by recombinant protein kinases.** A, time course of RGS9-1 phosphorylation by PKG (30 units/ml), PKA (50 units/ml), and Ca<sup>2+</sup>/CaM II kinase (0.8  $\mu$ g/ml). The RGS9-1 kinase activity was assayed by immunoblot using Ser<sup>475</sup> phosphate-specific antibody (A4) or a phosphocellulose method (graph) using a synthetic peptide that encompassed the identified Ser<sup>475</sup> phosphorylation site (KLDRRS<sup>475</sup>QLKKGLPPK) as described under "Materials and Methods." B, PKG, PKA, and Ca<sup>2+</sup>/CaM II kinase activities were measured by synthetic control peptides as described under "Materials and Methods." C, recombinant PKGI, PKGII, and ROS were immunoblotted with PKGI- and PKGII-specific antibodies. PKGI and PKGII are not present in bovine ROS.

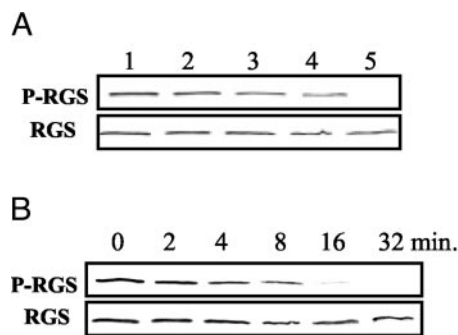


**FIG. 7. Dephosphorylation of endogenous phosphorylated RGS9-1.** A, dephosphorylation was carried out without (lane 1) or with the addition of PP2B (lane 2); PP2B with CaM and Ca<sup>2+</sup> (lane 3); PP1 (lane 4); or protein phosphatase 2A (lane 5). B, dephosphorylation time course of phosphorylated RGS9-1 by protein phosphatase 2A. Upper and lower immunoblots in both panels show P-RGS9-1 (A4) and RGS9-1 (D7), respectively.

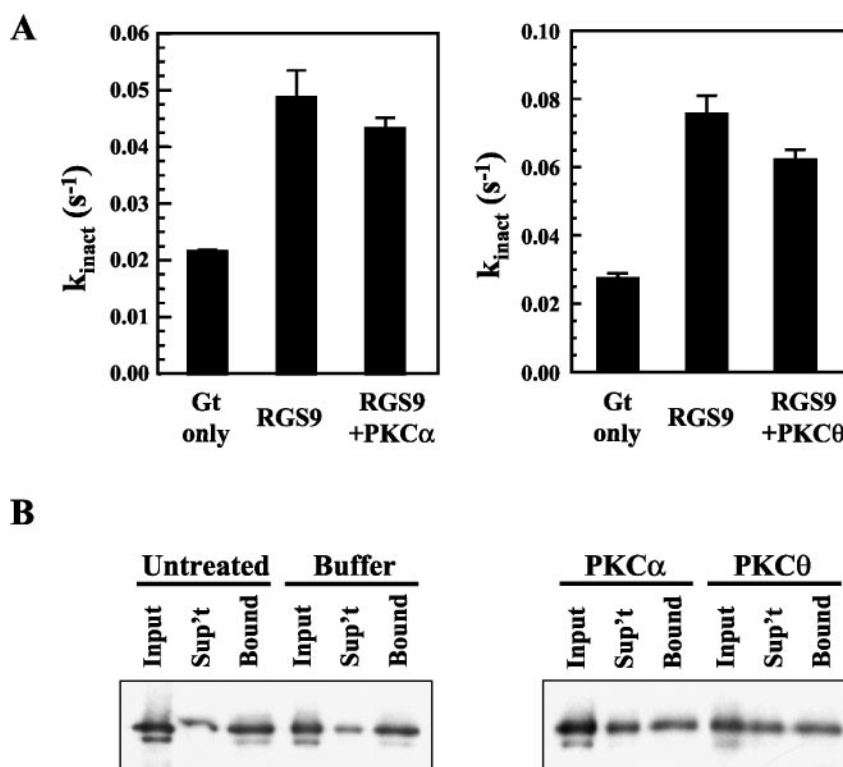
(data not shown). Subsequent heparin-Sepharose chromatography of the kinase fractions eluted from DEAE-Sepharose resulted in the important separation of three RGS9-1 kinase activity peaks (Fig. 3A), with peak 1 being more variable between preparations in terms of maximal activity. The small amounts of these kinases and the partial nature of the purification precluded us from direct sequence identification of these kinases; however, full separations of these activities allowed further biochemical characterization. In summary, using conventional column chromatography, we were able to identify three unique fractions of RGS9-1 kinase activity, suggesting the involvement of multiple

kinases in the phosphorylation of Ser<sup>475</sup> within RGS9-1.

**PS-dependent Stimulation of RGS9-1 Kinase(s)**—Next, we tested if the kinase activities obtained from the Heparin-Sepharose column were stimulated by common kinase modulators like cGMP; cAMP; DAG, PS, and Ca<sup>2+</sup>; PS, PMA, and Ca<sup>2+</sup>; CaM and Ca<sup>2+</sup>; and EGTA. Using the peptide as a substrate, we found that the activities of RGS9-1 kinases in peaks 2 and 3 were elevated in the presence of DAG, PS and Ca<sup>2+</sup>, with kinase peak 3 having the most dramatic increase (Fig. 3A). In fact, the total contribution of peak 3 to the RGS9-1 kinase activity increased from 40 to 77% upon stimulation, constituting the largest fraction of activity from these three peaks. On the other hand, when the full-length recombinant RGS9-1/G $\beta$ 5 was used as substrate, the activity of all three kinase peaks could be enhanced similarly by combination of PS, PMA, Ca<sup>2+</sup> or PS, DAG, and Ca<sup>2+</sup> (Fig. 3B). Previously, we suggested that the RGS9-1 kinase(s) may belong to the PKC family based on our finding that RGS9-1 phosphorylation can be inhibited by a PKC inhibitor, bisindolylmaleimide I (18). It is known that the conventional PKCs ( $\alpha$ ,  $\beta$ , and  $\gamma$ ) exhibit Ca<sup>2+</sup>/PS/DAG-stimulated kinase activity, whereas novel PKCs ( $\delta$ ,  $\epsilon$ ,  $\theta$ , and  $\eta$ ) exhibit only PS/DAG-stimulated activity, and atypical PKCs ( $\zeta$  and  $\iota/\lambda$ ) are Ca<sup>2+</sup>- and DAG-insensitive (29–31). The above data suggested that the kinases involved in RGS9-1 phosphorylation at Ser<sup>475</sup> could be members of the Ca<sup>2+</sup>/phospholipid-dependent PKC subfamily.

**Identification and Localization of PKC Isozymes**—Using immunoblot analysis with antibodies raised against recombinant PKC isozymes, we found that PKC $\alpha$ , PKC $\epsilon$ , and PKC $\theta$  are expressed in the ROS (Fig. 4B). In addition, PKC $\alpha$  and PKC $\theta$

FIG. 8. **Functional consequences of RGS9-1 phosphorylation.** A, GAP activities of RGS9-1 (RGS9) and PKC-phosphorylated RGS9 (RGS9 + PKC $\alpha$ , RGS9 + PKC $\theta$ ) were measured by single turnover assays in the presence of PDE $\gamma$ . B, binding of RGS9-1 (untreated), RGS9-1 incubated with kinase assay buffer and ATP (buffer), or RGS9-1 phosphorylated by PKC $\alpha$  or PKC $\theta$  to R9AP vesicles was measured as described under "Materials and Methods." Equal proportions of the binding reaction (input), supernatant after pelleting R9AP vesicles (*sup't*), and pelleted vesicles resuspended in SDS-sample buffer were loaded, and RGS9-1 in each fraction was detected by immunoblotting using polyclonal anti-RGS9-1c antiserum.



were detected in heparin-Sepharose isolated fraction 24 and 17, respectively (Fig. 4C). PKC $\alpha$  was previously implicated in phototransduction processes (32, 33). However, similar to results reported by Williams *et al.* (34), we were not able to localize PKC $\alpha$  to photoreceptor cells by immunocytochemical methods (data not shown). Immunostaining of the retina with a polyclonal antibody against PKC $\theta$  indicated immunoreactivity in the cones, which were identified with peanut agglutinin staining (Fig. 4A). Preincubation with immunoreactive peptide prior to staining abolished the PKC $\theta$  signal. The immunoblotting of ROS proteins also revealed the presence of PKC $\epsilon$  (Fig. 4B). However, this antigen was not detected in any fraction separated on the heparin-Sepharose column. This result was supported by the finding that PKC $\epsilon$  could not be extracted with high efficiency from the ROS under our conditions even by 1 M NH $_4$ Cl (data not shown). Along with previously published data (35–37), this result indicated that ROS PKC $\epsilon$  may be anchored to cytoskeleton proteins.

**Phosphorylation of RGS9-1 by PKC Isozymes**—Because of the presence of PKC $\alpha$  and PKC $\theta$  in the kinase activity peaks, we then compared the phosphorylation of RGS9-1 by the partially purified kinase peak fractions and by their corresponding recombinant PKC isozymes. Phosphorylation of RGS9-1 peptide by fraction 14 (possibly, in part, containing PKC $\epsilon$ ), fraction 17 (containing PKC $\theta$ ), and fraction 24 (containing PKC $\alpha$ ) showed similar kinetics to those of PKC $\epsilon$ , PKC $\theta$ , and PKC $\alpha$ , respectively (Fig. 5). Phosphorylation of full-length RGS9-1 by both the kinase peaks and the corresponding recombinant PKCs showed similar enhancement upon PS and Ca $^{2+}$  stimulation. Therefore, these data suggest that PKC $\alpha$ , PKC $\theta$ , and PKC $\epsilon$  are probably the kinases responsible for RGS9-1 phosphorylation.

The specificity of PKC phosphorylation of RGS9-1 may be partially determined by the membrane environment in which they normally interact. Although the predominant site in RGS9-1 phosphorylated by the endogenous kinases in ROS membranes is Ser $^{475}$ , and an RGS9-1 mutant lacking that site is not efficiently phosphorylated, both recombinant highly ac-

tive PKC $\alpha$  and PKC $\theta$  phosphorylate the S475A mutant of RGS9-1 almost as well as wild type RGS9-1 (data not shown). Thus, there are at least two potential sites for phosphorylation of RGS9-1 by PKC isozymes, and selection of these may be determined by the nature of association with membranes and other ROS proteins.

We also tested other kinases phosphorylated sequence corresponding to the RGS9-1 Ser $^{475}$  phosphorylation site (38). We compared PKG, PKA, and Ca $^{2+}$ /CaM II kinase for their abilities to phosphorylate recombinant RGS9-1 or its peptide (Fig. 6, A and B). The phosphorylation level by PKA and CaM kinase II was much lower than that by PKC isoforms. Although PKGI did show strong phosphorylation of RGS9-1, immunoblotting of different fractions with specific antibodies produced against PKGI and PKGII, together with immunocytochemistry (data not shown), did not provide any evidence for the presence of PKG in photoreceptor cells (Fig. 6C). With all three kinases, PKGI, PKA, and Ca $^{2+}$ /CaM II kinase, positive results were obtained with their specific peptides (Fig. 6B), indicating that all enzymes were reactive in our assays.

**Dephosphorylation of RGS9-1 by PP2A**—Since phosphorylation of endogenous RGS9-1 is light-dependent (18), both phosphorylation and dephosphorylation should be regulated processes. To identify the phosphatase responsible for dephosphorylation, we tested PP1, PP2A, and PP2B (Fig. 7). Using the Ser $^{475}$  phosphorylation-specific antibody A4, we found that PP2A was capable of removing the phosphate from Ser $^{475}$  (Fig. 7, lane 5), whereas neither PP1 nor PP2B could catalyze the dephosphorylation reaction efficiently. Importantly, PP2A was previously isolated from ROS (39–43). These findings suggest that PP2A is possibly the RGS9-1 phosphatase that can specifically dephosphorylate RGS9-1 at Ser $^{475}$ .

**Functional Consequences of RGS9-1 Phosphorylation**—RGS9-1 is the GTPase-accelerating protein for Gta $\alpha$ , and its GAP activity can be regulated by its association with ROS membranes through the interaction with its membrane anchor R9AP. To study the functional consequences of RGS9-1 phosphorylation, we therefore tested whether phosphorylation mod-

ulates the function of RGS9-1 by direct regulation of its GAP activity or by regulation of its R9AP-mediated membrane binding. When the GAP activities of RGS9-1 before and after phosphorylation by recombinant PKCs (PKC $\alpha$  or PKC $\theta$ ) were compared in the presence of the effector subunit PDE $\gamma$ , we found that phosphorylation slightly inhibited the GAP activity of RGS9-1 (Fig. 8A). These results were obtained in the absence of the membrane anchor for RGS9-1, R9AP. A more significant effect of PKC phosphorylation was found on binding to R9AP. We found that phosphorylation caused RGS9-1 to bind the R9AP vesicles much less tightly (Fig. 8B). Since membrane tethering of RGS9-1 by R9AP dramatically enhances the GAP activity RGS9-1,<sup>2</sup> this result indicated that phosphorylation of RGS9-1 may decrease its catalytic activity toward Gt $\alpha$  through dissociating the membrane complex between RGS9-1 and R9AP. Therefore, by modulating RGS9-1 GAP activity both directly and indirectly, phosphorylation of RGS9-1 by PKC isoforms could provide a regulatory mechanism for modifying the inactivation kinetics in phototransduction.

#### DISCUSSION

**Phosphorylation Occurs in Rods**—RGS9-1 is highly expressed in cone but is also present in rod photoreceptors cells (Fig. 1A) (16). To obtain additional evidence that the observed phosphorylation of RGS9-1 (18) occurs in rods, which are a readily accessible source for biochemical isolation, we measured RGS9-1 phosphorylation in transgenic mice lacking cones. We demonstrated that phosphorylation of RGS9-1 takes place in dark-adapted rods and then dephosphorylation occurs when mice are exposed to light. There were no significant differences between *Coneless* mice and wild type mice (Fig. 1B), strengthening the argument that RGS9-1 phosphorylation is taking place in rods.

**Multiple Forms of PKC Involved in the RGS9-1 Phosphorylation**—By purification of RGS9-1 kinase(s) from ROS extracts, we identified that multiple forms of PKC are involved in RGS9-1 phosphorylation at Ser<sup>475</sup>. PKCs constitute a protein family that displays lipid- and cofactor-stimulated kinase activity (44, 45). Three groups of PKC isozymes were identified that display unique requirements for Ca<sup>2+</sup>. The conventional PKCs encoded by  $\alpha$ ,  $\beta$ , and  $\gamma$  genes exhibit Ca<sup>2+</sup>/PS/DAG-stimulated kinase activity, whereas novel PKC $\delta$ ,  $\epsilon$ ,  $\theta$ , and  $\eta$  exhibit only PS/DAG-stimulated activity. The atypical PKC subfamily comprises the  $\zeta$  and  $\iota/\lambda$  isotypes, which are Ca<sup>2+</sup>- and DAG-insensitive.

PKC $\alpha$ ,  $\epsilon$ , and  $\theta$  were present in bovine ROS, and at least two of these kinases were found to be involved in RGS9-1 phosphorylation. They could be extracted with 1 M NH<sub>4</sub>Cl (Fig. 2A) from ROS membranes and separated on a heparin-Sepharose column (Fig. 3). Since PKCs are dependent upon PS for activity (46), it was important to test the heparin-separated activity profile in the presence of this cofactor (Fig. 3A). A combination of DAG, PS, and Ca<sup>2+</sup> or of PS, PMA, and Ca<sup>2+</sup> significantly elevated activity in fraction 24, as judged by rRGS9-1 (Fig. 3B) and RGS9-1 peptide phosphorylation (data not shown). Two other fractions did not show significant changes in RGS9-1 peptide phosphorylation, but a higher level of phosphorylation was detected when full-length rRGS9-1 was used. These data, combined with the fact that recombinant PKC $\alpha$ ,  $\epsilon$ , and  $\theta$  effectively catalyze phosphorylation of RGS9-1 on Ser<sup>475</sup> (Fig. 5), support the idea that these PKC isoforms are the enzymes involved in RGS9-1 phosphorylation.

Among all of the kinase candidates we tested, we also found that PKG robustly phosphorylated RGS9-1 at Ser<sup>475</sup> (Fig. 6), but PKA and Ca<sup>2+</sup>/CaM-dependent kinase II did not. However, we, as well as other groups, were not able to find any evidence of the presence of PKGI or PKGII isoforms in either purified

ROS or the outer segment of mouse photoreceptors.

**Localization of PKC Isozymes**—Although immunocytochemical methods were generally not successful in localizing PKC $\alpha$  in ROS of several species (34, 47–55), PKC $\alpha$  has been detected and purified from ROS (34, 56–58). For PKC $\theta$ , we found that it specifically localizes to COS (Fig. 4). Therefore, it is possible that the observed kinase activity in peak 2 resulted from the contamination of ROS by COS. Alternatively, it is also possible that immunoreactivity toward PKC $\theta$  is masked in ROS and that the enzyme is present in both COS and ROS or simply that PKC $\theta$  is present in much higher amounts in cones than in rods, as is the RGS9-1 complex. Moreover, the levels of peak 1 varied from preparation to preparation, suggesting variable extraction efficiency between experiments or contamination of ROS preparation by kinases from other retinal cells. Peak 1 could, in part, be due to the presence of PKC $\epsilon$ . It appears that PKC $\epsilon$  is tightly bound to membranes in ROS. Because commercially available antibody, although effective in immunoblotting, was not useful for immunolocalization, we were not able to localize this isoform in mouse retina sections. These findings are also consistent with a report suggesting that PKC $\alpha$ ,  $\beta$ I,  $\beta$ II,  $\gamma$ ,  $\delta$ ,  $\epsilon$ , and  $\zeta$  and another structurally unknown PKC subspecies are expressed in the retina (54).

Based on biochemical studies, PKC was suggested to be involved in several processes of phototransduction, including rhodopsin phosphorylation (33, 59). Phosphorylation of rhodopsin is involved in lowering the catalytic efficiency of photoactivated rhodopsin in the activation of Gt (60, 61). These authors suggest that most of the PKC in photoreceptor outer segments is of the conventional type and that most, if not all, of this conventional PKC activity comes from a novel isozyme(s) (34). Subsequent studies (62, 63) have not supported a physiologically significant role for PKC in rhodopsin phosphorylation. Further studies to resolve the role of PKCs in phototransduction, including phosphorylation of RGS9-1 will require a combination of biochemical experiments in conjunction with *in vivo* studies that take advantage of mouse genetics.

**Phosphatases and Dephosphorylation of RGS9-1**—Of the three most common enzymes, protein phosphatase 2A, dephosphorylates phosphorylated RGS9-1 at Ser<sup>475</sup>. Protein phosphatase 2A has been identified as one of the many enzymes dephosphorylating phosphorylated rhodopsin in ROS (39–43). This enzyme is not regulated by Ca<sup>2+</sup> or phospholipids. Therefore, the regulation of RGS9-1 phosphorylation is on the level of protein kinases.

**Unique RGS9-1 C-terminal Sequence and Its Kinase**—RGS9 belongs to the R7 RGS subfamily and is expressed in retina and brain as the spliced forms RGS9-1 and RGS9-2, respectively (7). The retina-specific human RGS9-1 contains 484 amino acid residues, whereas the larger form in the brain contains ~675 residues (14). Except for a unique C-terminal portion (difference begins at residue 467 in RGS9-2), both variants are identical. The 18-amino acid long tail characteristic for RGS9-1 was not found even in very closely related RGS sequences. The function of this unique sequence is still unknown. However, some data suggested its importance in the interactions of RGS9-1 with targets (10, 17, 65). As highlighted in the sequence alignment (Fig. 2B), the C-terminal part of RGS9-1 contains Ser<sup>475</sup> that is phosphorylated by PKC.

**Functional Consequences of RGS9-1 Phosphorylation**—PKC phosphorylation of RGS9-1 *in vitro* resulted in dramatic reduction in its affinity for its membrane anchor, R9AP (Fig. 8), which would be expected *in vivo* to reduce its catalytic activity toward Gt $\alpha$ . Although the GAP activity of RGS9-1 originates from its RGS domain (1) and the R9AP-mediated membrane targeting originates from its N-terminal domain (17), neither of

which are adjacent in the linear amino acid sequence to Ser<sup>475</sup>, it is known that both the C- and N-terminal domains are important for regulation of RGS domain GAP activity by PDE $\gamma$  (10, 65), and both have been implicated along with R9AP in RGS9-1 membrane association (17, 64, 66). Therefore, our observation that phosphorylation of Ser<sup>475</sup> further affected the function of RGS9-1 supports the idea that the function of RGS9-1 is tightly controlled on multiple levels. Furthermore, RGS9-1 phosphorylation was found to be regulated by light *in vivo*, with the highest phosphorylation levels detected in dark-adapted animals and the lowest in light-adapted animals. If phosphorylation indeed reduces RGS9-1 GAP activity *in vivo*, then light would be expected to stimulate the activity of RGS9-1, potentially providing a novel mechanism contributing to light adaptation.

**Acknowledgments**—We thank Dr. J. Nathans (Johns Hopkins University) and Dr. J. Chen (Southern California University) for *Coneless* mice and GCAP1/GCAP2 knockout mice, respectively, Dr. M. Uhler (University of Michigan) for the PKGII kinase construct and anti-PKGII antibody, Jing Huang for flat mount immunocytochemistry, and Dr. Volker Gerke for comments on the manuscript. We are grateful to Yunie Kim and Matthew Batten for help during the manuscript preparation.

## REFERENCES

- He, W., Cowan, C. W., and Wensel, T. G. (1998) *Neuron* **20**, 95–102
- Ross, E. M., and Wilkie, T. M. (2000) *Annu. Rev. Biochem.* **69**, 795–827
- De Vries, L., Zheng, B., Fischer, T., Elenko, E., and Farquhar, M. G. (2000) *Annu. Rev. Pharmacol. Toxicol.* **40**, 235–271
- Arshavsky, V., and Bownds, M. D. (1992) *Nature* **357**, 416–417
- Chen, C. K., Burns, M. E., He, W., Wensel, T. G., Baylor, D. A., and Simon, M. I. (2000) *Nature* **403**, 557–560
- McBee, J. K., Palczewski, K., Baehr, W., and Pepperberg, D. R. (2001) *Prog. Retin Eye Res.* **20**, 469–529
- Cowan, C. W., He, W., and Wensel, T. G. (2000) *Prog. Nucleic Acids Res. Mol. Biol.* **65**, 341–359
- Snow, B. E., Krumins, A. M., Brothers, G. M., Lee, S. F., Wall, M. A., Chung, S., Mangion, J., Arya, S., Gilman, A. G., and Siderovski, D. P. (1998) *Proc. Natl. Acad. Sci. U. S. A.* **95**, 13307–13312
- Witherow, D. S., Wang, Q., Levay, K., Cabrera, J. L., Chen, J., Willars, G. B., and Slepak, V. Z. (2000) *J. Biol. Chem.* **275**, 24872–24880
- He, W., Lu, L., Zhang, X., El-Hodiri, H. M., Chen, C. K., Slep, K. C., Simon, M. I., Jamrich, M., and Wensel, T. G. (2000) *J. Biol. Chem.* **275**, 37093–37100
- Makino, E. R., Handy, J. W., Li, T., and Arshavsky, V. Y. (1999) *Proc. Natl. Acad. Sci. U. S. A.* **96**, 1947–1952
- Levay, K., Cabrera, J. L., Satpaev, D. K., and Slepak, V. Z. (1999) *Proc. Natl. Acad. Sci. U. S. A.* **96**, 2503–2507
- Kovoor, A., Chen, C. K., He, W., Wensel, T. G., Simon, M. I., and Lester, H. A. (2000) *J. Biol. Chem.* **275**, 3397–3402
- Zhang, K., Howes, K. A., He, W., Bronson, J. D., Pettenati, M. J., Chen, C., Palczewski, K., Wensel, T. G., and Baehr, W. (1999) *Gene (Amst.)* **240**, 23–34
- Rahman, Z., Gold, S. J., Potenza, M. N., Cowan, C. W., Ni, Y. G., He, W., Wensel, T. G., and Nestler, E. J. (1999) *J. Neurosci.* **19**, 2016–2026
- Cowan, C. W., Fariss, R. N., Sokal, I., Palczewski, K., and Wensel, T. G. (1998) *Proc. Natl. Acad. Sci. U. S. A.* **95**, 5351–5356
- Hu, G., and Wensel, T. G. (2002) *Proc. Natl. Acad. Sci. U. S. A.* **99**, 9755–9760
- Hu, G., Jang, G. F., Cowan, C. W., Wensel, T. G., and Palczewski, K. (2001) *J. Biol. Chem.* **276**, 22287–22295
- Nair, K. S., Balasubramanian, N., and Slepak, V. Z. (2002) *Curr. Biol.* **12**, 421–425
- Balasubramanian, N., Levay, K., Keren-Raifman, T., Faurobert, E., and Slepak, V. Z. (2001) *Biochemistry* **40**, 12619–12627
- Witt, J. J., and Roskoski, R., Jr. (1975) *Anal. Biochem.* **66**, 253–258
- Papermaster, D. S. (1982) *Methods Enzymol.* **81**, 48–52
- Uhler, M. D. (1993) *J. Biol. Chem.* **268**, 13586–13591
- Laemmli, U. K. (1970) *Nature* **227**, 680–685
- Angleson, J. K., and Wensel, T. G. (1994) *J. Biol. Chem.* **269**, 16290–16296
- Soucy, E., Wang, Y., Nirenberg, S., Nathans, J., and Meister, M. (1998) *Neuron* **21**, 481–493
- Sokal, I., Li, N., Verlinde, C. L., Haeseleer, F., Baehr, W., and Palczewski, K. (2000) *Biochim. Biophys. Acta* **1498**, 233–251
- Polans, A., Baehr, W., and Palczewski, K. (1996) *Trends Neurosci.* **19**, 547–554
- Nishizuka, Y. (2001) *Alcohol Clin. Exp. Res.* **25**, 3–7
- Nishizuka, Y. (1995) *FASEB J.* **9**, 484–496
- Nishizuka, Y. (1992) *Science* **258**, 607–614
- Wolbring, G., and Schnetkamp, P. P. (1995) *Biochemistry* **34**, 4689–4695
- Newton, A. C., and Williams, D. S. (1993) *Trends Biochem. Sci.* **18**, 275–277
- Williams, D. S., Liu, X., Schlamp, C. L., Ondek, B., Jaken, S., and Newton, A. C. (1997) *J. Neurochem.* **69**, 1693–1702
- Cenni, V., Doppler, H., Sonnenburg, E. D., Maraldi, N., Newton, A. C., and Toker, A. (2002) *Biochem. J.* **363**, 537–545
- Mochly-Rosen, D. (1995) *Science* **268**, 247–251
- Mochly-Rosen, D., Smith, B. L., Chen, C. H., Disatnik, M. H., and Ron, D. (1995) *Biochem. Soc. Trans.* **23**, 596–600
- Kemp, B. E., Pearson, R. B., and House, C. M. (1991) *Methods Enzymol.* **201**, 287–304
- Palczewski, K., Hargrave, P. A., McDowell, J. H., and Ingebritsen, T. S. (1989) *Biochemistry* **28**, 415–419
- Palczewski, K., McDowell, J. H., Jakes, S., Ingebritsen, T. S., and Hargrave, P. A. (1989) *J. Biol. Chem.* **264**, 15770–15773
- Palczewski, K., Farber, D. B., and Hargrave, P. A. (1991) *Exp. Eye Res.* **53**, 101–105
- Fowles, C., Akhtar, M., and Cohen, P. (1989) *Biochemistry* **28**, 9385–9391
- King, A. J., Andjelkovic, N., Hemmings, B. A., and Akhtar, M. (1994) *Eur. J. Biochem.* **225**, 383–394
- Nishizuka, Y. (1988) *Nature* **334**, 661–665
- Mellor, H., and Parker, P. J. (1998) *Biochem. J.* **332**, 281–292
- Parker, P. J., Stabel, S., and Waterfield, M. D. (1984) *EMBO J.* **3**, 953–959
- Wood, J. G., Hart, C. E., Mazzei, G. J., Girard, P. R., and Kuo, J. F. (1988) *Histochem. J.* **20**, 63–68
- Yoshida, Y., Huang, F. L., Nakabayashi, H., and Huang, K. P. (1988) *J. Biol. Chem.* **263**, 9868–9873
- Negishi, K., Kato, S., and Teranishi, T. (1988) *Neurosci. Lett.* **94**, 247–252
- Suzuki, S., and Kaneko, A. (1990) *Vis. Neurosci.* **5**, 223–230
- Cuenca, N., Fernandez, E., and Kolb, H. (1990) *Brain Res.* **532**, 278–287
- Usuda, N., Kong, Y., Hagiwara, M., Uchida, C., Terasawa, M., Nagata, T., and Hidaka, H. (1991) *J. Cell Biol.* **112**, 1241–1247
- Zhang, D. R., and Yeh, H. H. (1991) *Vis. Neurosci.* **6**, 429–437
- Fujisawa, N., Ogita, K., Saito, N., and Nishizuka, Y. (1992) *FEBS Lett.* **309**, 409–412
- Koistinaho, J., and Sagar, S. M. (1994) *Neurosci. Lett.* **177**, 15–18
- Newton, A. C. (1993) *Methods Neurosci.* **16**, 261–269
- Kelleher, D. J., and Johnson, G. L. (1985) *J. Cyclic Nucleotide Protein Phosphor. Res.* **10**, 579–591
- Wolbring, G., and Cook, N. J. (1991) *Eur. J. Biochem.* **201**, 601–606
- Greene, N. M., Williams, D. S., and Newton, A. C. (1997) *J. Biol. Chem.* **272**, 10341–10344
- Palczewski, K. (1997) *Eur. J. Biochem.* **248**, 261–269
- Palczewski, K., and Benovic, J. L. (1991) *Trends Biochem. Sci.* **16**, 387–391
- Chen, C. K., Burns, M. E., Spencer, M., Niemi, G. A., Chen, J., Hurley, J. B., Baylor, D. A., and Simon, M. I. (1999) *Proc. Natl. Acad. Sci. U. S. A.* **96**, 3718–3722
- Xiong, W., Nakatani, K., Ye, B., and Yau, K. (1997) *J. Gen. Physiol.* **110**, 441–452
- Lishko, P. V., Martemyanov, K. A., Hopp, J. A., and Arshavsky, V. Y. (2002) *J. Biol. Chem.* **277**, 24376–24381
- Skiba, N. P., Martemyanov, K. A., Elflein, A., Hopp, J. A., Bohm, A., Simonds, W. F., and Arshavsky, V. Y. (2001) *J. Biol. Chem.* **276**, 37365–37372
- He, W., Melia, T. J., Cowan, C. W., and Wensel, T. G. (2001) *J. Biol. Chem.* **276**, 48961–48966